Synthesis and Properties of Covalently Bonded Layered Silicates/Polyimide (BTDA-ODA) Nanocomposites

Chyi-Ming Leu, Zhen-Wei Wu, and Kung-Hwa Wei*

Department of Materials Science and Engineering, National Chiao Tung University, Hsinchu, Taiwan 30049, R.O.C.

Received January 15, 2002. Revised Manuscript Received April 8, 2002

Covalently bonded layered silicates/polyimide (BTDA-ODA) nanocomposites have been synthesized from γ-(aminopropyl)triethoxysilane (APTS) grafted kenyaite and poly(amic acid). The existence of covalent bonds between APTS and silicates and between APTS and the dianhydride end groups of the polymer have been confirmed by solid-state ^{13}C and ^{29}Si nuclear magnetic resonance and infrared spectroscopy, respectively. The thermal, mechanical, and moistureabsorption retardation properties of these nanocomposites were found to improve substantially over those of neat BTDA-ODA. In particular, a maximum increase of 36 °C in the degradation temperature and a maximum reduction of 54% in moisture absorption are displayed by these nanocomposites.

Introduction

Hybrid organic/inorganic nanocomposites have attracted a great deal of attention because of their intricate microstructures and enhanced properties.[1−2] For example, layered silicate/polymer nanocomposites can be synthesized either by dispersing organic-modified montmorillonite in polymers[3−21] or via in situ polymerization of monomers.[22−23] The critical step in both processes involves converting originally hydrophilic montmorillonite, which contains negatively charged layered silicates held together by metal ions, into partially hydrophobic and hydrophilic (amphiphilic) species. By replacing the metal ions in the intergallery of silicates with protonated organic molecules (swelling agent) such as alkyl or aromatic ammonium, the layered silicate aggregates intercalate and become miscible with organic macromolecules. The intercalated silicates then allow larger-sized macromolecules to diffuse into the intergallery and cause further intercalation or exfoliation. If a functional group present in the swelling agent is able to react with the chain end of the macromolecule, then the ionicly bonded, polymer-tethered layered silicate can form. With this approach, we found a substantial increase in the thermal and mechanical properties of such an ionicly bonded system over that of neat polymer.[18−19] However, if the nanocomposites were formed by covalent bonding between polymers and layered silicates, the interfacial strength between these two dissimilar materials would become stronger and further enhance their thermal stability and moistureabsorption retardation properties. To our knowledge, there is only one study concerning the covalent bond approach in layered silicates/polymer hybrid synthesis.[24]

In the present study, we chose a hydrothermally synthesized Na-kenyaite ($Na_2Si_{22}O_{45}\cdot 10H_2O$),[25−27] which contains negatively charged layered polysilicates, constituted by SiO_4 tetrahedra,[28,29] for the source of layered silicates. Upon acidification, the Na-kenyaite is converted to H-kenyaite, with surface OH groups able to form covalent bonds with surfactants. The modification of H-kenyaite requires polar solvents and surfactants. Because of the silanol groups in the interlayer regions of silicates of H-kenyaite, these layered silicates swell

* To whom correspondence should be addressed. Phone: 886-35-731871. Fax: 886-35-724727. E-mail: khwei@cc.nctu.edu.tw.

(1) Okada, A.; Usuki, A. *Mater. Sci. Eng.* **1995**, *C3*, 109.
(2) Giannelis, E. P. *Adv. Mater.* **1996**, *8*, 29.
(3) Usuki, A.; Kawasumi, M.; Kojima, Y.; Okada, A.; Kurauchi, T.; Kamigaito, O. *J. Mater. Res.* **1993**, *8*, 1174.
(4) Usuki, A.; Kojima, Y.; Kawasumi, M.; Okada, A.; Fukushima, Y.; Kurauchi, T.; Kamigaito, O. *J. Mater. Res.* **1993**, *8*, 1179.
(5) Kojima, Y.; Usuki, A.; Kawasumi, M.; Okada, A.; Fukushima, Y.; Kurauchi, T.; Kamigaito, O. *J. Mater. Res.* **1993**, *8*, 1185.
(6) Wang, M. S.; Pinnavaia, T. J. *Chem. Mater.* **1994**, *6*, 468.
(7) Messersmith, P. B.; Giannelis, E. P. *Chem. Mater.* **1994**, *6*, 1719.
(8) Lan, T.; Kaviratna, P. D.; Pinnavaia, T. J. *Chem. Mater.* **1995**, *7*, 2144.
(9) Wang, Z.; Pinnavaia, T. J. *Chem. Mater.* **1998**, *10*, 3771.
(10) Chen, T. K.; Tien, Y. I.; Wei, K. H. *J. Polym. Sci., Part A: Polym. Chem.* **1999**, *37*, 2225.
(11) Chen, T. K.; Tien, Y. I.; Wei, K. H. *Polymer* **2000**, *41*, 1345.
(12) Yano, K.; Usuki, A.; Okada, A.; Kurauchi, T.; Kamigaito, O. *J. Polym. Sci., Part A: Polym. Chem.* **1993**, *31*, 2493.
(13) Yano, K.; Usuki, A.; Okada, A. *J. Polym. Sci., Part A: Polym. Chem.* **1997**, *35*, 2289.
(14) Lan, T.; Kaviratna, P. D.; Pinnavaia, T. J. *Chem. Mater.* **1994**, *6*, 573.
(15) Tien, Y. I.; Wei, K. H. *Macromolecule* **2001**, *34*, 9045.
(16) Tyan, H. L.; Liu, Y. C.; Wei, K. H. *Polymer* **1999**, *40*, 4877.
(17) Tyan, H. L.; Liu, Y. C.; Wei, K. H. *Chem. Mater.* **1999**, *11*, 1942.
(18) Tyan, H. L.; Wei, K. H.; Hsieh, T. E. *J. Polym. Sci. Polym. Phys.* **2000**, *38*, 2873.
(19) Tyan, H. L.; Leu, C. M.; Wei, K. H. *Chem. Mater.* **2001**, *13*, 222.
(20) Tyan, H. L.; Wu, C. Y.; Wei, K. H. *J. Appl. Polym. Sci.* **2001**, *81*, 1742.
(21) Jiang, L. Y.; Leu, C. M.; Wei, K. H. *Adv. Mater.* **2002**, *14*, 426.
(22) Zeng, C.; Lee, L. J. *Macromolecule* **2001**, *34*, 4098.
(23) Weimer, M. W.; Chen, H.; Giannelis, E. P.; Sogah, D. Y. *J. Am. Chem. Soc.* **1999**, *121*, 1615.
(24) Isoda, K.; Kuroda, K.; Ogawa, M. *Chem. Mater.* **2000**, *12*, 1702.
(25) Lagaly, G.; Beneke, K.; Weiss, A. *Am. Mineral.* **1975**, *60*, 642.
(26) Beneke, K.; Lagaly, G. *Am. Mineral.* **1977**, *62*, 763.
(27) Beneke, K.; Lagaly, G. *Am. Mineral.* **1983**, *68*, 818.
(28) Brindley, G. W. *Am. Mineral.* **1969**, *54*, 1583.
(29) Schwieger, W.; Heidemann, D.; Bergk, K.-H. *Rev. Chim. Miner.* **1985**, 22, 639.

10.1021/cm0200240 CCC: $22.00 © 2002 American Chemical Society
Published on Web 06/04/2002

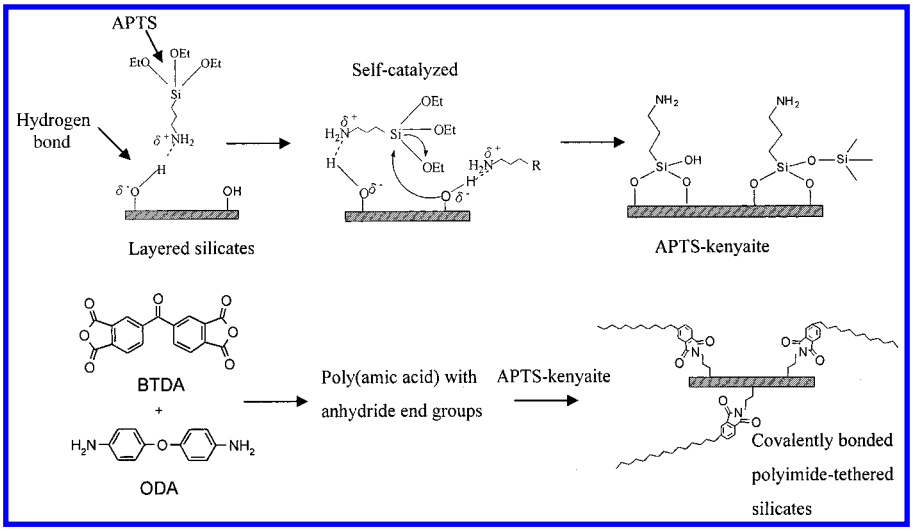

Figure 1. Schematic drawing of the formation process of covalently bonded polyimide tethered layered silicates.

in the presence of polar organic solvents such as *N*-methylformamide, dimethyl sulfoxide and *N*,*N*-dimethylacetamide (DMAc).[30] Next, the interlamellar covalent-bond grafting of γ-(aminopropyl)triethoxysilane (APTS)[24,31−34] (which is a frequently used surfactant in silica gel[35,36]) on layered silicates was carried out in DMAc. APTS can first hydrogen bond with the surface hydroxyl groups of layered silicates and then form siloxane bonds with layered silicates through self-catalyzed condensation at elevated temperatures. After this modification, the kenyaite is denoted as APTS-kenyaite. When APTS-kenyaite is mixed with poly(amic acid) (BTDA-ODA type) containing an anhydride end group, the amino group of APTS-kenyaite can react with the anhydride end group of poly(amic acid) to form covalently bonded polymer tethered silicates. A schematic drawing of the formation process of polymer tethered APTS-kenyaite is presented in Figure 1. In this study, the thermal, mechanical and moistureabsorption properties of the covalently bonded layered silicate/polyimide nanocomposites are investigated.

Experimental Section

Materials. Fumed silica (surface area = 200 m^2/g), analytical reagent grade of NaOH, HCl, γ-(aminopropyl)triethoxysilane, and *N*,*N*-Dimethylacetamide (DMAc) were obtained from Aldrich. 3,3′,4,4′-Benzophenone tetracarboxylic dianhydride (BTDA) and 4,4′-oxydianiline (ODA) were purchased from TCI in Tokyo, Japan.

Synthesis of Na-Kenyaite and APTS-Kenyaite. Na-kenyaite was synthesized via a hydrothermal method in our laboratory. A suspension of amorphous silica, sodium hydroxide, and water at a molar ratio of 3:1:200 was sealed in a Teflon-lined reactor at 150 °C for 48 h. The product was washed with a dilute aqueous NaOH solution and dried in air. H-kenyaite was obtained by an ion exchange reaction of 10.00 g of kenyaite and 4.00 g of 37.5 wt % HCl aqueous solution in 1.0 L of DI water after being stirred at room temperature for 5 days. A total of 1.20 g of the H-kenyaite was suspended in 20.0 mL of anhydrous DMAc under nitrogen purge at 25 °C for 1 h. Then, 2.0 mL of γ-(aminopropyl)triethoxysilane was added to the suspension and stirred for 1 h. After the treatment, the suspension was stirred under nitrogen purge at 110 °C for 48 h and then filtered and washed with DMAc and acetone. The precipitated solid was dried in a vacuum at 80 °C for 12 h.

Model Compound Study by APTS-Kenyaite-BTDA. APTS-kenyaite-BTDA was synthesized from APTS-kenyaite and BTDA in DMAc, and used as a model compound study for APTS-kenyaite/polyimide. A total of 0.50 g of APTS-kenyaite was put into a three-neck flask containing 24.62 g of DMAc under nitrogen purge at 25 °C and stirred for 1 h. Then, 0.50 g of BTDA was added into the flask, and it stirred for 12 h. After the treatment, the mixture was filtered and washed with DMAc. The precipitated solid was put in an air-circulation oven at 100, 150, 200, and 300 °C for 1 h and then at 350 °C for 0.5 h to ensure a complete imidization.

Preparation of APTS-Kenyaite/Polyimide (BTDA-ODA) Nanocomposites. Poly(amic acid) (PAA) was synthesized by first putting 2.94 g (14.70 mmol) of ODA into a three-neck flask containing 24.62 g of DMAc under nitrogen purge at 25 °C. Then, after ODA was completely dissolved in DMAc, 4.83 g of (15.00 mmol) of BTDA, which was divided into three batches, was added to the flask batch-by-batch with a time interval of 0.5 h between batches. When BTDA was completely dissolved in DMAc, the solutions were stirred for 1 h, and a viscous PAA solution was obtained. Different concentrations of APTS-kenyaite in DMAc were prepared by putting 0, 0.08, 0.23, 0.39, and 0.55 g of APTS-kenyaite in 16.20 g DMAc and by mixing each of them for 12 h. These APTS-kenyaite suspensions were then mixed with the PAA to obtain APTS-kenyaite/PAA in DMAc. The final solid content of PAA in DMAc was 16 wt % determined by dividing the total weight of BTDA and ODA with the total weight of BTDA, ODA, and DMAc. The intrinsic viscosity of poly(amic acid) in DMAc at 30 °C is 0.99 dL/g. These APTS-kenyaite/PAA mixtures were cast on glass slides by a doctor blade and were subsequently placed in a vacuum oven at 30 °C for 48 h before the imidization step. Imidization of APTS-kenyaite/PAA was carried out by putting the samples in an air-circulation oven at 100, 150, 200, and 300 °C for 1 h and then at 350 °C for 0.5 h to ensure a complete imidization.

Characterization. The X-ray diffraction study was carried out by a MAC Science MXP18 X-ray diffractometer (30 kV, 20 mA) with copper target at a scanning rate of 4 °/min. The ^{13}C and ^{29}Si solid-state CPMAS NMR spectra were recorded on a DSX400 NMR spectrometer. Infrared spectra of KBr disks

(30) Lagaly, G.; Beneka, K.; Weiss, A. *Am. Mineral.* **1975**, *60*, 650.
(31) Ruiz-Hitzky, E.; Rojo, J. M. *Nature* **1980**, *287*, 28.
(32) Ruiz-Hitzky, E.; Rojo, J. M.; Largaly, G. *Colloid Polym. Sci.* **1985**, *263*, 1025.
(33) Ogawa, M.; Okutomo, S.; Kuroda, K. *J. Am. Chem. Soc.* **1998**, *120*, 7361.
(34) Shimojima, A.; Mochizuki, D.; Kuroda, K. *Chem. Mater.* **2001**, *13*, 3603.
(35) Chiang, C.; Liu, N.; Koenig, J. L. *J. Colloid Interface Sci.* **1982**, *86*, 26.
(36) Vrancken, K. C.; Van Der Voort, P.; Gillis-D'Hamers, I.; Vansant, E. F. Daelemans, F. *J. Chem. Soc., Faraday Trans.* **1992**, *88*(21), 3197.

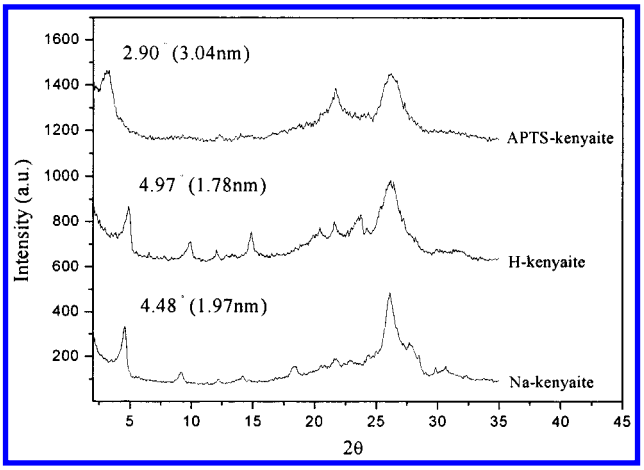

Figure 2. X-ray diffraction curves of Na-kenyaite, H-kenyaite, and APTS-kenyaite.

were recorded on a Nicolet Protégé-460 Fourier transform spectrophotometer. Scanning electron micrographs were obtained by a TOPCON ABT-150S micrograph with an accelerating voltage of 20 kV. The stack sizes of 1 wt % of layered silicates in water were obtained with an Ultrafine Particle Size Analyzer of Honeywell.

Samples for the transmission electron microscopy (TEM) study were prepared by first putting APTS-kenyaite/BTDA-ODA films into epoxy capsules and then curing the epoxy at 70 °C for 48 h in a vacuum oven. Then, the cured epoxy samples were microtomed with Leica Ultracut Uct into about 90 nm-thick slices. Subsequently, a layer of carbon about 3 nm thick was deposited onto these slices and placed on mesh 200 copper nets for TEM observation. The TEM instrument used was a JEOL-2000 FX, with an acceleration voltage of 200 kV. The thermal gravimetric and thermal transition analyses of APTS-kenyaite/BTDA-ODA nanocomposite films were carried out with a Du Pont TGA 2950 and a Du Pont DSC 2910 at a heating rate of 20 °C/min with nitrogen purge. The coefficient of thermal expansion (CTE) measurements for the films were carried out using a Du Pont TMA 2940 (film probe) at a heating rate of 10 °C/min in a nitrogen atmosphere. The tensile properties of APTS-kenyaite/BTDA-ODA films were measured according to the specifications of ASTM D882−88 at a crosshead speed of 2 mm/min. Moisture absorption measurements of thin polyimide nanocomposite films (~15 μm) were carried out in an environmental chamber at 30 °C for 72 h under 85% relative humidity. The percentage of moisture absorption was calculated based on eq 1:

$$\text{moisture absorption (\%)} = [(W_1\text{-}W_0)/W_0] \times 100\% \quad (1)$$

Here, W_1 and W_0 represent the moisture-absorbed weight and the dried weight of APTS-kenyaite/BTDA-ODA, respectively.

Results and Discussion

Figure 2 shows the X-ray diffraction patterns of three different stages of kenyaite. The X-ray diffraction patterns of Na-kenyaite and H-kenyaite are consistent with previous reports,[22−24] with *d*-spacings of layered silicates of 2.0 and 1.8 nm, respectively. In the case of APTS-kenyaite, the peak at $2\theta = 2.9°$, *d*-spacing = 3.0 nm, resulted from the diffraction of the (001) crystal surfaces of the layered silicates, suggesting that the interlayer distance of silicates has increased.

Chemical structure evidence of the grafting of APTS onto the layered silicates in H-kenyaite can be determined from their solid-state ^{13}C and ^{29}Si NMR spectra, as shown in Figures 3 and 4, respectively. In Figure 3, the peaks at 9.5, 26.3, and 43.3 ppm are due to the

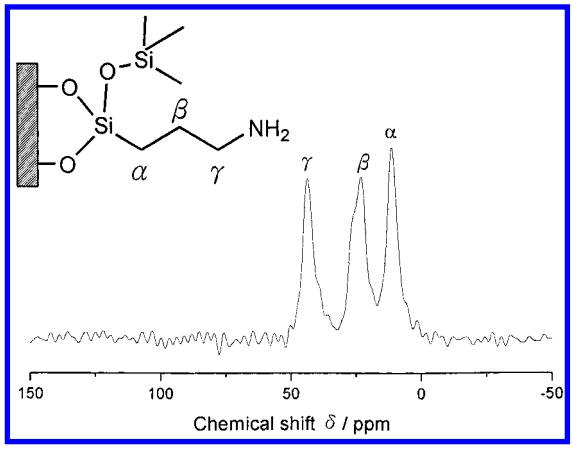

Figure 3. ^{13}C NMR spectrum of APTS-kenyaite.

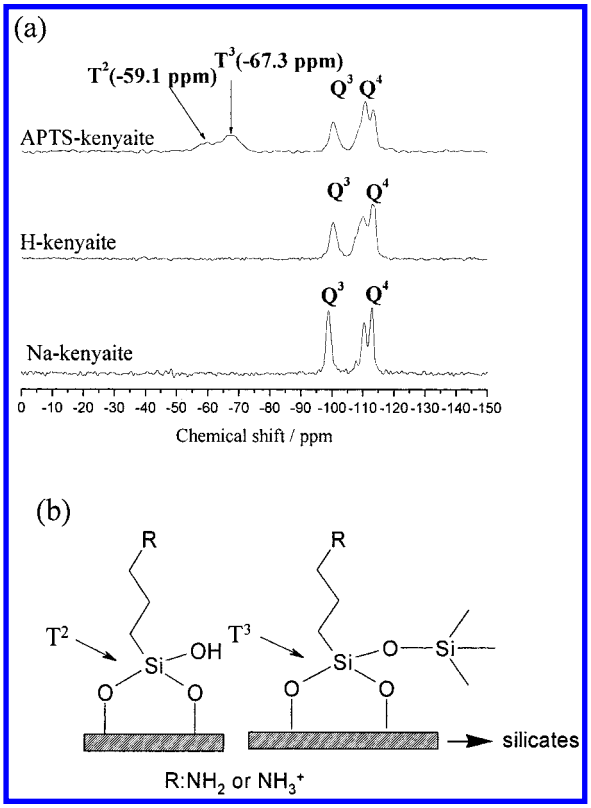

Figure 4. (a) ^{29}Si CP/MAS NMR spectra of Na-kenyaite, H-kenyaite, and APTS-kenyaite and (b) structures of APTS-kenyaite.

α-CH, *β*-CH, and *γ*-CH groups of APTS, respectively, confirming the existence of APTS structures. As compared to the α-CH peak of pure APTS, which is located at 7.9 ppm, the change in the chemical shift implies the attachment of APTS onto the layered silicates. Furthermore, Figure 4a display two peaks at −98.2 and −114.0 ppm (Q^3 and Q^4) that are due to the chemical structures of $[Si(OSi)_3OH]$ and $[Si(OSi)_4]$ in layered silicates of kenyaite, respectively. The two additional ^{29}Si peaks at −59.1 and −67.3 ppm (T^2 and T^3) in Figure 4a are caused by the APTS groups attached to the layered silicates surface consisting of $-[Si(OSi)_2OH]$ and $-[Si(OSi)_3]$, respectively. The T^2 and T^3 structures are shown in Figure 4b. The spectra information from ^{13}C and ^{29}Si solid-state NMR provide direct evidence of covalent bonding between APTS and layered silicates in H-kenyaite.

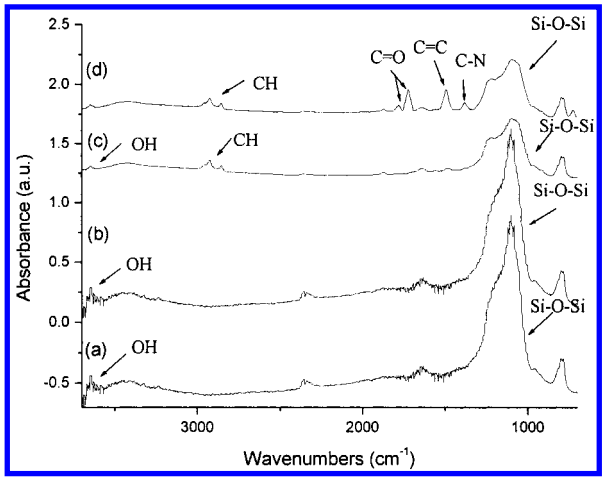

Figure 5. IR spectra of (a) Na-kenyaite, (b) H-kenyaite, (c) APTS-kenyaite, and (d) APTS-kenyaite-BTDA.

Figure 5 shows the IR spectra of Na-kenyaite, H-kenyaite, APTS-kenyaite, and APTS-kenyaite-BTDA. For APTS-kenyaite, the intensity of the 3650 cm^{-1} band caused by the OH stretching vibration of the free silanol group is weaker than that for the case of pure H-kenyaite. Moreover, the appearance of two new bands between 2700 and 3000 cm^{-1}, due to C−H stretching vibration in the APTS-kenyaite case, indicates the attachment of APTS to H-kenyaite. The moles of APTS grafted to kenyaite can be determined by the difference in the weight loss of H-kenyaite and APTS-kenyaite. On the other hand, the mole fraction of the Si−OH group on silicates can be found in the ratio of the area under peak Q^3 and Q^4 and is $^1/_4$ in this case. Assuming all Si−OH groups appeared on the surface of kenyaite, the fraction of APTS bonded Si−OH groups in kenyaite can be deduced by dividing the moles of grafted APTS with the moles of Si−OH group on silicates, which turns out be about 66%. In the model compound study, the APTS-kenyaite was mixed with BTDA in DMAc for reaction, and then the solvent in the mixture was evaporated. The IR spectrum of the resultant mixture contains peaks at 1380, 1720, and 1780 cm^{-1} that are caused by C−N stretching, asymmetric imide C═O stretching, and symmetric imide C═O stretching, respectively. Hence, the NH_2 functional groups in APTS-kenyaite are able to react with the dianhydride end groups of poly(amic acid).

Figure 6 shows the SEM micrographs of kenyaite with different modifications. Na-kenyaite and H-kenyaite form spherical nodules resembling rosettes. The rosette is exfoliated into smaller structures after silylation by APTS molecules. The platelets display slightly wrapped structures. The stack sizes of Na-kenyaite, H-kenyaite, and APTS-kenyaite in Figure 6 are between 600 and 800 nm. For hydrophilic Na-kenyaite, the stack size from the SEM is lightly larger than that dispersed in water (300−700 nm) as determined from particle size analysis. The stack sizes of hydrophobic H-kenyaite and APTS-kenyaite found from the particle size analysis are 3.3−5.1 μm and 1.5−2.2 μm, respectively.

There is no X-ray diffraction peak between $2\theta = 2°$ and 10° for BTDA-ODA containing 1.0, 3.0, 5.0, and 7.0 wt % APTS-kenyaite, indicating that the d spacing between silicates is greater than 3 nm in these cases, but the silicates are not necessarily exfoliated. The

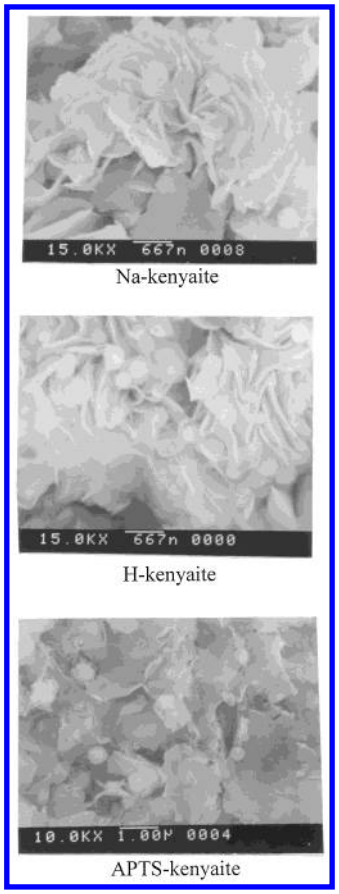

Figure 6. SEM micrographs of Na-kenyaite, H-kenyaite, and APTS-kenyaite.

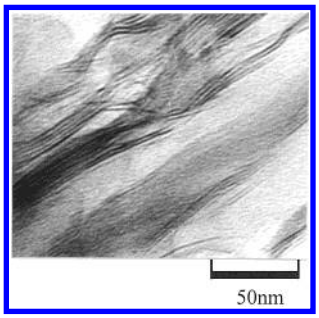

Figure 7. TEM micrographs of 3 wt % APTS-kenyaite/polyimide(BTDA-ODA).

dispersion model of silicates can be found in the transmission electron microscopy examination of a cross section of APTS-kenyaite/BTDA-ODA, as shown in Figure 7. The TEM micrographs show intercalated as well as exfoliated domains. The distance between the silicate layers in some domains of BTDA-ODA containing 3.0 wt % APTS-kenyaite (dark lines) is larger than 6 nm. The thermal properties of APTS-kenyaite/BTDA-ODA nanocomposites for different compositions are given in Table 1. The thermal degradation temperatures (Td) of the nanocomposites increased slightly with the amount of APTS-kenyaite; a maximum increase of 36 °C occurred in the case of BTDA-ODA containing 7.0 wt % APTS-kenyaite, as compared to that of pure BTDA-ODA. The increase in Td resulted from the fact that the covalently bonded nanosized layered silicates, about 700 nm long and 2 nm thick, are able to sustain high temperature and to retard the heat diffusion into polyimide. The glass transition temperatures (Tg) of

Table 1. Thermal Properties of Covalently Bonded APTS-Kenyaite/BTDA-ODA Nanocomposites at Different Compositions

amount of APTS-kenyaite in BTDA-ODA	Td[a] (°C)	Tg (°C)	CTE $(ppm/°C)_{50-250\ °C}$
0 (neat BTDA-ODA)	585	279	43.7
1.0 wt %	600	280	38.6
3.0 wt %	617	282	35.5
5.0 wt %	619	285	33.2
7.0 wt %	621	287	32.4

[a] Td degradation temperature at 5 wt % loss.

Table 2. Tensile Mechanical Properties of Covalently Bonded APTS-Kenyaite/BTDA-ODA Nanocomposites at Different Compositions

amount of APTS-kenyaite in BTDA-ODA	Young's modulus (GPa)	max. stress (MPa)	max. elongation (%)
0 (neat BTDA-ODA)	2.15 ± 0.07	95.4 ± 3.1	7 ± 1
1.0 wt %	2.21 ± 0.07	98.4 ± 2.2	9 ± 1
3.0 wt %	2.30 ± 0.07	109.1 ± 3.6	10 ± 1
5.0 wt %	2.41 ± 0.08	110.4 ± 3.6	9 ± 1
7.0 wt %	2.73 ± 0.09	113.1 ± 3.7	8 ± 1

APTS-kenyaite/BTDA-ODA also increased slightly with the amount of APTS-kenyaite. This phenomenon can be explained by the fact that the main-chain motion of BTDA-ODA might be affected by the covalently bonded layered silicates. The in-plane CTE of APTS-kenyaite/BTDA-ODA nanocomposite films are given in Table 1. The CTE are substantially lower than that of the pristine BTDA-ODA and also decreased slightly with the amount of the APTS-kenyaite.

Table 2 summarizes the tensile mechanical properties of these nanocomposites. The Young's modulus and maximum stresses of those nanocomposites increased slightly with the amount of silicates, but the elongation-at-break of these nanocomposites showed little change. The increases in the modulus of the nanocomposites were apparently caused by the addition of stiff layered silicates. The increases in maximum stresses for these nanocomposites suggest that the interfacial strength between layered silicates and BTDA-ODA was better than that between BTDA-ODA molecules, quite possibly because of covalent bonding.

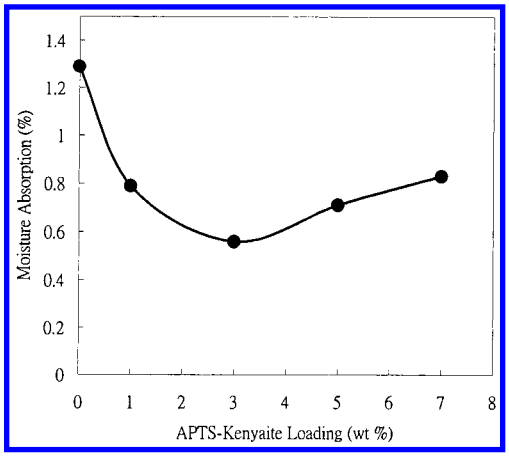

Figure 8. Moisture absorption properties of APTS-kenyaite/BTDA-ODA nanocomposites at different compositions.

The moisture absorption values of APTS-kenyaite/BTDA-ODA nanocomposites at different compositions are given in Figure 8. The moisture absorption of the nanocomposites reached a minimum value of 0.60 wt % at 3.0 wt % silicates content, as opposed to 1.30 wt % by neat BTDA-ODA, revealing a 54% reduction. This phenomenon can be explained by the fact that the amount of moisture absorption by layered silicates/BTDA-ODA is controlled by two competing factors.

Table 3. Properties of Ionicly Bonded Layered Silicates/Polyimide

		Td (°C)	Tg (°C)	CTE (ppm/°C)	Young's modulus (GPa)	max. stress (MPa)	max. elongation (%)	moisture absorption (%)
a	PPD-mont/PMDA-ODA							
	0	618	366		2.45	88.2	10	
	1	626	368		2.95	93.4	11	
	2	631	369	*b*	3.15	94.8	11	*b*
	3	637	369		3.27	96.7	12	
	5	643	370		3.34	99.5	13	
	7	643	369		3.46	101.4	13	
c	ODA-mont/BTDA-ODA	585	276	44	1.35	75.3	7	1.3
	0	595	277	39	1.78	75.7	7	1.0
	1 wt %	607	279	34	2.66	93.7	8	0.8
	3 wt %	610	279	33	3.22	105.4	8	1.0
	5 wt %							
d	$12CH_3$-mont/PMDA-ODA			57				2.9
	0			54				
	1 wt %			46				2.8
	2 wt %	*b*	*b*	44	*b*	*b*	*b*	
	3 wt %			42				42
	5 wt %			35				35
	8 wt %							
e	$12CH_3$-mont/BTDA-ODA		305	73				
	0		305	73				
	1 wt %	*b*	295	68	*b*	*b*	*b*	*b*
	3 wt %		305	62				
	6 wt %		264	62				
	9 w t%		284	60				
	11 wt %							

[a] Tyan, H. L. *Chem. Mater.* **1999**, *11*, 1942. [b] Not available. [c] Tyan, H. L. *J. Polym. Sci., Part B: Polym. Phys.* **2000**, *38*, 2873. Tyan, H. L. *J. Appl. Polym. Sci.* **2001**, *81*,1742. [d] Yano, K. J. *Polym. Sci., Part A: Polym. Chem.* **1993**, *31*, 2493. [e] Magaraphan, R. *Comp. Sci. Tech.* **2001**, *61*, 1253.

Because moisture absorption experiments are carried out in thermodynamic equilibrium, the polyimide in the intergallery of the layered silicates may have absorbed a much smaller amount of water than in the pristine polyimide case because of the barrier effect of silicates. The second factor is that some water molecules physically absorb to defects of tetrahedral SiO_4. Hence, this physical adsorption of water molecules onto silicates will increase as the amount of silicates increases.

For a comparison, the properties of ionicly bonded polyimide/layered silicates by a few studies are given in Table 3. For the thermal degradation temperatures, the maximum increase in Td of the APTS-kenyaite/BTDA-ODA case is larger than that of PPD-mont/PMDA-ODA and ODA-mont/BTDA-ODA cases (36 °C vs 25 °C).[17,18,20] For the in-plane CTE, the decreases of CTE of BTDA-ODA or PMDA-ODA[13] containing 5 wt % modified layered silicates are about 25%, with the exception of $12CH_3$-mont/BTDA-ODA (15%).[37] For the tensile mechanical properties of these nanocomposites, the Young's modulus and the maximum stress of the APTS-kenyaite/BTDA-ODA, PPD-mont/PMDA-ODA, and ODA-mont/BTDA-ODA increased with the amount of silicates, despite different types of bonding. The maximum elongations of these nanocomposites, however, remain about the same as that of pure polyimide. The reduction of the moisture absorptions in APTS-kenyaite/BTDA-ODA case is more pronounced than that in ODA-mont/BTDA-ODA case.

(37) Magaraphan, R.; Lilayuthalert, W.; Sirivat, A.; Schwank, J. W. *Comput. Sci. Technol.* **2001**, *61*, 1253.

Concluding Remarks

The covalent bond approach in forming layered silicates/polyimide nanocomposites resulted in enhanced thermal, mechanical, and moistureabsorption retardation properties over those of neat polyimide. Additionally, this approach might provide a new type of nanocomposite with better thermal and moistureabsorption retardation properties than those of ionicly bonded polymer-tethered nanocomposites.

Acknowledgment. We appreciate the financial support provided by the National Science Council through Project NSC 90-2216-E−009-017.

CM0200240